A Landau free energy for diblock copolymers with compressibility difference between blocks

ARTICLE *in* THE JOURNAL OF CHEMICAL PHYSICS · SEPTEMBER 2003

Impact Factor: 2.95 · DOI: 10.1063/1.1599278

1 AUTHOR:

Junhan Cho
Dankook University
67 PUBLICATIONS **625** CITATIONS

SEE PROFILE

A Landau free energy for diblock copolymers with compressibility difference between blocks

Junhan Cho

Department of Polymer Science & Engineering, and Hyperstuructured Organic Materials Research Center, Dankook University, San-8, Hannam-dong, Yongsan-gu, Seoul 140-714, Korea

A new Landau free energy is derived for diblock copolymers of incompatible pairs based on the recently developed compressible random-phase approximation (RPA) analysis. Finite compressibility of each block is generally allowed. The inhomogeneity of each block density and free volume is analyzed in the weak segregation regime. Free volume inhomogeneity fluctuates in two ways; one represents compressibility difference between blocks and the other stands for the screening of unfavorable cross-contacts. It is shown from the Landau energy that a continuous transition, observed in a symmetric block copolymer either incompressible or with no compressibility difference, disappears provided that one block is more compressible. Microphase transitions and their pressure response of commonly used diblock copolymers are calculated and compared with experimental results. A Flory-type interaction parameter χ_{cRPA}, which is suggested from the effective second-order vertex function in the free energy, is shown to be useful owing to its compressible nature in understanding of the phase behavior of various copolymers.

I. INTRODUCTION

Block copolymers from two or more incompatible polymers have been known to exhibit a microphase separation from a disordered state to an ordered state upon cooling, which is called the upper order-disorder transition (UODT) behavior. The UODT behavior is driven by the unfavorable interactions between dissimilar monomers comprising a given block copolymer. A number of nanoscale ordered structures have been identified up to now. There are classical morphologies such as body-centered cubic spheres (bcc), hexagonally packed cylinders (hex), and lamellar (lam) structures. Recently found morphologies such as bicontinuous gyroid, hexagonally perforated lamellae, and the latest non-cubic triply periodic structures are categorized as complex morphologies.[1,2]

There have been in recent decades extensive theoretical developments to analyze the microphase separation behavior and transitions between equilibrium microstructures for molten block copolymers or systems containing block copolymers in weak to strong segregation regime.[2] Most of the theories developed so far are based on the common assumption of system incompressibility. Among them, Leibler suggested a Landau mean-field analysis based on the random-phase approximation (RPA) for weakly segregating diblock copolymer melts near spinodals.[3,4] It was revealed that asymmetric block copolymers undergo a general sequence of transitions from a disordered state to a metastable bcc, then to a hex, and then finally to a lam morphology upon cooling. A symmetric one was shown to exhibit a continuous transition from the disordered state to the lam morphology. Leibler's mean-field theory was later corrected by Fredrickson and Helfand, [5] and then by Mayes and Olvera de la Cruz [6] in a more general way to include concentration fluctuation effects. It was shown that for a

copolymer of finite molecular weight the continuous transition disappears and the direct transition to the hex or lam morphology is possible.

In the past decade, there have emerged a different class of theories that take finite compressibility into consideration in a given block copolymer system. Those theories are based on the so-called compressible RPA approaches. Freed and co-workers were the first to incorporate finite compressibility into the incompressible RPA by allowing for vacancy. [7] Other theories have also been formulated using vacancies as a pseudosolvent in the incompressible treatment. [8] Pair correlation functions and spinodals from the compressible RPA theories were used to explain a newly found microphase separation behavior, which is induced inversely by heating and thus referred to as the lower disorder-order transition (LDOT). Some diblock copolymer melts from polystyrene and lower alkyl polymethacrylates, [9] and from polystyrene and poly(vinyl methyl ether) [10] exhibited such LDOT behavior. The existence of LDOT indeed necessitates compressibility because it is considered to be driven by difference in volume fluctuations between constituent polymers. [11]

In the mean time, a new and unique compressible RPA theory was recently introduced by the present author. [12-16] Akcasu's general compressible RPA formalism, [17] which discards the Lagrange multiplier for the incompressibility constraint in RPA calculations, was employed for the first time instead of the pseudosolvent technique. Finite compressibility was incorporated into the theory through effective RPA interaction fields, which is obtained from an off-lattice equation-of-state (EOS) model by Cho and Sanchez (CS) in Appendix A. [12,18] Pair and many-body correlation functions, and the corresponding vertex functions of the Landau expansion of the free energy in packing density fluctuations for diblock copolymer melts were formulated up

to quartic order. [13,14] Compressible Landau free energy densities treating of classical microphase morphologies were then obtained in the following two extreme cases: firstly for LDOT diblock copolymer melts with favorable cross-contact interactions that microphase separate upon heating due to compressibility difference between blocks; [13] secondly for UODT copolymer melts with the identical compressibility for both blocks, whose microphase separation is induced by the unfavorable energetics. [14] The transition temperatures, equilibrium microphase morphologies, and the order of transition were discussed with the help of such Landau mean-field energies. It was found that the continuous transition for a symmetric copolymer vanishes in the former case, but is restored in the latter systems with the identical compressibility for both blocks. In all cases, the general sequence of microphase transition (disorder $\rightarrow$ bcc $\rightarrow$ hex $\rightarrow$ lam) was sustained as segregation is progressed.

The objective of the present article is to generalize the latter Landau free energy by allowing finite compressibility difference between blocks in order to analyze the phase behavior of most block copolymers which are UODT systems. It is of our particular interest to study the responses of UODT systems relevant to compressibility such as the pressure dependence of transition temperatures, as pressure is always involved in processing conditions and thus designing self-assembled microstructures. The inhomogeneity of free volume in UODT systems induced by microphase separation is considered to fluctuate in two ways. Excess free volume is to be present either at the domain of more compressible constituent or at the interface between domains to screen unfavorable cross interactions. A reasonable treatment of the packing density and free volume fluctuations then results in the desired analytical Landau free energy density for the copolymers. In this mean-field study, UODT systems are shown to belong to Ising

universality class with a continuous transition in the symmetric case if there is no compressibility difference between blocks. However, the presence of compressibility difference is shown to remove the critical behavior for symmetric copolymers even in the mean-field situation, which assures our previous result on the LDOT systems.

The present theory, based on the mean-field approach, possesses certain limitations. Chains in a given system are assumed ideal. Therefore, chain-stretching effects are not considered. [19] Concentration fluctuation effects are also ignored. A leading harmonic is only employed to describe a given morphology, so that only classical morphologies are considered here. Improvement in the present theory by correcting its limitations is expected to give substantial changes in the mean-field phase diagram.

Several hypothetical and real diblock copolymer systems are considered here for our present analysis. Those copolymers reveal a diversified microphase transition behavior from conventional to anomalous upon pressurization. The molecular origin for such diversified behavior is explained in a clear and succinct manner. In addition, an effective Flory-type interaction parameter, χ_{cRPA}, is to be extracted naturally from the approximate quadratic term of the formulated Landau free energy. It is shown that the behavior of χ_{cRPA}, which carries the compressible nature of a given copolymer, is helpful in understanding of the phase behavior of the systems of our interest.

Our treatment for finite compressibility in block copolymers through the CS model can also be applied to simulation studies. Maurits et al. recently performed the dynamic mean-field density functional simulations, which were derived from the generalized time-dependent Ginzburg-Landau theory, to investigate coarse-grained morphology dynamics in a compressible diblock copolymer system. [20] In their approach, thermodynamic forces in a given system were obtained from a suitable free

energy functional, with which several EOS models were combined in order to describe the system compressibility. The CS model can then be readily incorporated into Maurits et al.'s simulations to give a substantial improvement in their work because of the proven accuracy of the CS model in correlating volume data of various polymers. [18]

II. NEW LANDAU FREE ENERGY

Consider a system of A-*b*-B diblock copolymers with r_i monomers of the *i*th component, where *i* = 1 and 2 correspond to A and B, respectively, to have the overall size r_T ($=\sum_i r_i$). All the monomers are assumed to have the identical diameter σ. The volume fraction ϕ_i of the *i*th component is then defined as $\phi_i \equiv r_i / r_T$. The system is allowed to be compressible: there is free volume in the system. We denote as η_i the global packing density of *i*-monomers that implies the fraction of system volume occupied by all the monomers of the *i*th component. The $\eta_i(\vec{r})$ represents the local packing density of such monomers at a position $\vec{r}$. Phase segregation in the system can be probed by considering the average packing density fluctuations, or the order parameter ψ_i, for the *i*-monomers. The order parameter ψ_i is defined as

$$\psi_i(\vec{r}) \equiv \langle \delta\eta_i(\vec{r}) \rangle = \langle \eta_i(\vec{r}) - \eta_i \rangle \qquad (1)$$

where the brackets in Eq. (1) imply the thermal average. In a Landau mean-field approach, the free energy for the system can be expanded as a series in the order parameter ψ_i as

$$F - F_0 = \frac{1}{\beta}\sum_{n=2}^{\infty}\frac{1}{n!}\int d\vec{q}_1 \cdots d\vec{q}_n \Gamma^{(n)}_{i_1 \cdots i_n}(\vec{q}_1, \cdots, \vec{q}_n)\psi_{i_1}(\vec{q}_1)\cdots\psi_{i_n}(\vec{q}_n) \qquad (2)$$

where the F_0 implies the free energy in a disordered state and $\beta = 1/kT$ has its usual meaning. In the above equation, the Fourier component of ψ_i has been used for the convenience of subsequent manipulation of the free energy. The $\vec{q}_i$ in Eq. (2) denotes physically the scattering vector as phase segregation is often investigated by radiation scattering techniques. The coefficient $\Gamma^{(n)}_{i_1 \cdots i_n}$ is commonly known as the *n*th-order vertex function. Such vertex functions based on the compressible RPA in connection with the CS model are explicitly written in Appendix B.

For the analysis of compressible UODT diblock copolymer systems, we perform a simple transformation of the order parameters in Eq. (1) into the following ones. [14]

$$\overline{\psi}_1 \equiv \frac{1}{2\eta}[\psi_1 - \psi_2] \qquad (3)$$

$$\overline{\psi}_2 \equiv \psi_1 + \psi_2 \qquad (4)$$

where the subscript *i* in $\overline{\psi}_i$ now indicates the two new order parameters, not the block component. In Eq. (3), η denotes the total packing density satisfying $\eta = \eta_1 + \eta_2$. The η_i is indeed equated to $\phi_i \eta$. It is easily seen that $\eta_1 + \eta_2 = 1 - \eta_f$, where η_f implies the fraction of free volume in the system. The $-\overline{\psi}_2$ then becomes identical to the average fluctuations in free volume fraction, $\langle \delta\eta_f \rangle$, because $\psi_1 + \psi_2 = -\langle \delta\eta_f \rangle$. The inhomogeneity of free volume is, therefore, probed through $\overline{\psi}_2$. These new order

parameters are convenient in the case of UODT systems. It can be said that $\overline{\psi}_2$ goes to zero as free volume is completely squeezed out. In such a case, $\overline{\psi}_1$ becomes the only order parameter left to be equal to simply ψ_1. The compressible RPA then converges to the incompressible case so that a direct comparison of the present analysis with that by Leibler[3] is possible. The vertex functions can be redefined in accord with the new order parameters as

$$\Gamma^{(n)}_{i_1\cdots i_n}(\vec{q}_1,\cdots,\vec{q}_n)\psi_{i_1}(\vec{q}_1)\cdots\psi_{i_n}(\vec{q}_n)=\overline{\Gamma}^{(n)}_{i_1\cdots i_n}(\vec{q}_1,\cdots,\vec{q}_n)\overline{\psi}_{i_1}(\vec{q}_1)\cdots\overline{\psi}_{i_n}(\vec{q}_n) \qquad (5)$$

In Appendix B, the explicit mathematical expressions are given for the new vertex functions. It should be perceived that both $\Gamma^{(n)}$ and $\overline{\Gamma}^{(n)}$ are vanishing unless $\sum_{i=1}^{n}\vec{q}_i=0$.

As microphase segregation develops, each component of the copolymer fluctuates in its concentration. The ordered pattern is simply described as the superposition of plane waves or harmonics. The free energy expansion in Eq. (2) is approximated to the sum containing only the most important contributions from the fastest growing waves with wavelength q^*.[3,21] The observed ordered structures are then represented by a set of n wave vectors $\vec{Q}_i$'s (i = 1, …, n), whose lengths are all q^*. There need six and three wave vectors for bcc and hex morphologies, respectively, and one wave vector for lam morphology. Those wave vectors are tabulated elsewhere.[3,13] Free volume possesses preference for a more compressible block if there is compressibility difference between blocks. Free volume then acts as a selective solvent. We intuitively expect that the excess free volume is present either at the more compressible

component or at the interface between two incompatible polymers in order to screen the unfavorable interactions. The fluctuations of free volume can thus be divided into two terms ($\overline{\psi}_2 \equiv \zeta + \xi$). Those associated with ζ stands for the compressibility difference, where ζ fluctuates with the wave number $\left|\vec{Q}_i\right|$. The remaining part ξ of $\overline{\psi}_2$ fluctuates with the wave number $2\left|\vec{Q}_i\right|$, which implies the screening effects at the interfaces. The order parameters to describe a given microphase morphology can, therefore, be parameterized as

$$\overline{\psi}_1(\vec{r}) = 2 \cdot \frac{1}{\sqrt{n}} \overline{\psi}_n(1) \sum_{k=1}^{n} \cos\left[\vec{Q}_k \cdot \vec{r} - \varphi_k(1)\right] \tag{6}$$

$$\zeta(\vec{r}) = 2 \cdot \frac{1}{\sqrt{n}} \zeta_n \sum_{k=1}^{n} \cos\left[\vec{Q}_k \cdot \vec{r} - \varphi_\zeta\right] \tag{7}$$

$$\xi(\vec{r}) = 2 \cdot \frac{1}{\sqrt{n}} \xi_n \sum_{k=1}^{n} \cos\left[2\vec{Q}_k \cdot \vec{r} - \varphi_\xi\right] \tag{8}$$

where $\overline{\psi}_n(1)/\sqrt{n}$, $\zeta_n/\sqrt{n}$, $\xi_n/\sqrt{n}$ and $\varphi_n(1), \varphi_\zeta, \varphi_\xi$ indicate the amplitudes and the phase angles, respectively, for the order parameters $\overline{\psi}_1$, ζ, and ξ. Figure 1 depicts the plot of such intuitively expected schematic behavior of the order parameters along the direction perpendicular to the lamellar layers as an illustration.

The Landau free energy can now be written in the power series of order parameters. Dividing the energy into quadratic, cubic, and quartic terms as $\delta F = \delta F_2 + \delta F_3 + \delta F_4$ yields

$$\beta\delta F_2 = \overline{\Gamma}_{11}^{(2)}\overline{\psi}_n(1)^2 + 2\overline{\Gamma}_{12}^{(2)}\overline{\psi}_n(1)\zeta_n e^{i[\varphi-\varphi_\zeta]} + \overline{\Gamma}_{22}^{(2)}\zeta_n^2 + \overline{\Gamma}_{22}^{(2)}(2q^*)\xi_n^2 \tag{9}$$

$$\begin{aligned}\beta\delta F_3 = {} & \overline{a}_n\overline{\Gamma}_{111}^{(3)}(1)\cdot\overline{\psi}_n(1)^3\sum_{\{\varphi\}} e^{i[\varphi(1)+\varphi(2)+\varphi(3)]} + \\ & \overline{a}_n\left(\overline{\Gamma}_{112}^{(3)}(1)+\overline{\Gamma}_{121}^{(3)}(1)+\overline{\Gamma}_{211}^{(3)}(1)\right)\overline{\psi}_n(1)^2\zeta_n\sum_{\{\varphi\}} e^{i[\varphi(1)+\varphi(2)+\varphi_\zeta]} + \\ & c_n\left(\overline{\Gamma}_{112}^{(3)}+\overline{\Gamma}_{121}^{(3)}+\overline{\Gamma}_{211}^{(3)}\right)\overline{\psi}_n(1)^2\xi_n e^{i[\varphi+\varphi-\varphi_\xi]}\end{aligned} \tag{10}$$

$$\beta F_4 = \sum_{\{h_1,h_2\}}\overline{b}(h_1,h_2)\cdot\overline{\Gamma}_{1111}^{(4)}(h_1,h_2)\overline{\psi}_n(1)^4 e^{i[\varphi(1)+\varphi(2)+\varphi(3)+\varphi(4)]} \tag{11}$$

The selection of terms in Eqs. (9)-(11) is based on the condition that $\sum\vec{q}_i = 0$. Therefore, there is no quadratic term coupled with ξ_n because $\vec{Q}_i$ and $-2\vec{Q}_i$ do not cancel out. For the cubic and quartic terms, the lowest-order coupled vertex functions are only chosen as it is perceived that the free volume inhomogeneity is far smaller than the inhomogeneity of each block density. The numerical coefficient $\overline{a}_n$ associated with $\overline{\Gamma}_{111}^{(3)}(1)$ and $\overline{\Gamma}_{112}^{(3)}(1)$, which are evaluated in the case that the three wave vectors form an equilateral triangle, is given as

$$\overline{a}_n = \frac{1}{3!}\frac{12}{\left(\sqrt{n}\right)^3} \text{ for bcc } (n=6) \text{ or hex } (n=3);\ \ \overline{a}_n = 0 \text{ for lam morphology} \tag{12}$$

The c_n associated with $\overline{\Gamma}_{112}^{(3)}$ and the other two, which involve two $\vec{Q}_i$'s and one $-2\vec{Q}_i$, is given as

$$c_n = \frac{1}{3!}\frac{12}{\left(\sqrt{6}\right)^3}, \frac{1}{3!}\frac{6}{\left(\sqrt{3}\right)^3}, \text{ and } \frac{2}{3!} \text{ for bcc, hex, and lam morphology, respectively} \tag{13}$$

The set of numbers (h_1, h_2) for $\overline{\Gamma}_{1111}^{(4)}$ defines the relative angles between four wave

vectors. The coefficients $\bar{b}(h_1,h_2)$ depend on the morphologies and the corresponding sets of vectors, as shown in the prior publications. [3,13]

The procedure in minimizing the free energy needs to take several steps starting from the quadratic term. For the convenience, we take the A-block is less compressible than B-block. It will be shown later that $\Gamma_{11}<\Gamma_{22}$ in this case. As $\overline{\Gamma}_{12}=\eta(\Gamma_{11}-\Gamma_{22})/2<0$, it is seen that $\varphi-\varphi_\zeta=0$ in order to minimize the free energy. This result implies that ζ is in phase with $\overline{\psi}_1$ ($\propto[\psi_1-\psi_2]$). As $\overline{\psi}_2$ is the negative of free volume inhomogeneity, -ζ represents the free volume fluctuations due to the compressibility difference. Therefore, more compressible component B possesses excess free volume, as is harmonious with our intuition. It is typical that the negativity of $\overline{\Gamma}^{(3)}_{111}(1)$ yields $\varphi(1)+\varphi(2)+\varphi(3)=0$. These two conditions on the phase angles give $\varphi(1)+\varphi(2)+\varphi_\zeta=-\varphi(3)+\varphi_\zeta=0$. The $\overline{\Gamma}^{(3)}_{112}$ and the other two in front of $\overline{\psi}_n(1)^2\xi_n$ are also negative. This procedure yields $\varphi+\varphi-\varphi_\xi=0$, which is again harmonious with our notion that the free volume fluctuations for screening have a half period because of two interfaces over one period of microstructure patterns. Finally, the sum of phase angles associated with $\overline{\Gamma}^{(4)}_{1111}(h_1,h_2)$ can be shown just to vanish. [3,13] Considering all the relations for the sums of phase angles gives the following expression of the Landau free energy:

$$\begin{aligned}\beta\delta F=&\overline{\Gamma}^{(2)}_{11}\overline{\psi}_n(1)^2+2\overline{\Gamma}^{(2)}_{12}\overline{\psi}_n(1)\zeta_n+\overline{\Gamma}^{(2)}_{22}\zeta_n^2+\overline{\Gamma}^{(2)}_{22}(2q^*)\xi_n^2\\&-\frac{\eta a_n}{r_T}\overline{\psi}_n(1)^3+\Delta\overline{\psi}_n(1)^2\zeta_n+\Pi\overline{\psi}_n(1)^2\xi_n+\frac{\eta b_n}{r_T}\overline{\psi}_n(1)^4\end{aligned}\qquad(14)$$

where a_n and b_n are identical with α_n and β_n (Eqs. (V-10), (11), (14), (15), and

(26) in ref 3) for a proper microphase morphology, respectively, in the Landau free energy by Leibler for incompressible UODT diblock copolymer melts. Two new coefficients, Δ and Π, can be written as

$$\Delta = k_n \cdot \bar{a}_n \cdot \left(\overline{\Gamma}^{(3)}_{112}(1) + \overline{\Gamma}^{(3)}_{121}(1) + \overline{\Gamma}^{(3)}_{211}(1) \right) \tag{15}$$

$$\Pi = c_n \left(\overline{\Gamma}^{(3)}_{112} + \overline{\Gamma}^{(3)}_{121} + \overline{\Gamma}^{(3)}_{211} \right) \tag{16}$$

where k_n = 4, 1, and 0 for bcc, hex, and lam morphology, respectively, and c_n is already given.

The Landau free energy in Eq. (14) can be further manipulated to yield the following conditions for ζ_n and ξ_n to minimize the free energy:

$$\zeta_n = -\frac{\overline{\Gamma}^{(2)}_{12}}{\overline{\Gamma}^{(2)}_{22}} \overline{\psi}_n(1) - \frac{\Delta}{2\overline{\Gamma}^{(2)}_{22}} \overline{\psi}_n(1)^2 \tag{17}$$

$$\xi_n = -\frac{\Pi}{2\overline{\Gamma}^{(2)}_{22}(2q^*)} \overline{\psi}_n(1)^2 \tag{18}$$

Putting Eqs. (17) and (18) into Eq. (14) gives the final expression for the desired Landau free energy to analyze microphase equilibria as

$$\begin{aligned} \beta\delta F = & \left[\overline{\Gamma}_{11} - \frac{\overline{\Gamma}^2_{12}}{\overline{\Gamma}_{22}} \right] \cdot \overline{\psi}_n(1)^2 \\ & - \left[\frac{\eta a_n}{r_T} + \frac{\Delta \overline{\Gamma}_{12}}{\overline{\Gamma}_{22}} \right] \overline{\psi}_n(1)^3 + \left[\frac{\eta b_n}{r_T} - \frac{\Delta^2}{4\overline{\Gamma}^{(2)}_{22}} - \frac{\Pi^2}{4\overline{\Gamma}^{(2)}_{22}(2q^*)} \right] \overline{\psi}_n(1)^4 \end{aligned} \tag{19}$$

Equation (18) shows that ξ_n is of order $\overline{\psi}_n(1)^2$. In order to make ζ_n being of the same order, an additional condition that $\left|\overline{\Gamma}_{12}^{(2)}\right| \le \left(|\Delta|/2\right)\cdot\overline{\psi}_n(1)$ is necessary, which is satisfied if the compressibility difference between blocks in UODT systems is small enough. The requirement that the Landau free energy is expanded only up to the order of $\overline{\psi}_n(1)^4$ is thus fulfilled. It should be noted that Π or Δ ~O(r_T^{-1}), and $\overline{\Gamma}_{22}^{(2)}$ ~ O(1). Therefore, the terms with Π^2 or Δ^2 are overwhelmed by $\eta b_n / r_T$ for high polymers as b_n ~ O(1). The order-disorder and order-order transitions are now to be determined by the minimization of Eq. (19) with respect to the only remaining $\overline{\psi}_n(1)$.

III. CALCULATION OF PHASE DIAGRAMS

The formulated Landau free energy is now applied to various UODT diblock copolymers to determine their phase behavior. To characterize a block component, one needs several molecular parameters based on the CS model in Appendix A. Those parameters include the self-interaction parameter $\overline{\varepsilon}_{ii}$, the monomer diameter σ_i, and the chain size r_i for homopolymers and the parameter $\overline{\varepsilon}_{ij}$ for cross interaction between different polymers. In Table I, the molecular parameters for four hypothetical polymers are tabulated. Those are carefully selected for us to characterize the phase behavior of most of the known UODT systems. Our present analysis assumes an identical monomer diameter σ for all constituents, so it is fixed to 4.04 Å. The chain sizes r_i will be provided later.

Prior to the calculation of phase diagram for various cases of UODT diblock copolymers, the physical meaning of $\overline{\Gamma}_{12}^{(2)}$ should be discussed. The Γ_{ij} is

approximated in the compressible RPA to the combination of the correlation function S_{ij}^{0} for noninteracting Gaussian chains and the interaction field W_{ij} as $\Gamma_{ij} = S_{ij}^{0^{-1}} + \beta W_{ij}$. The interaction field W_{ij}, formulated from the CS model, is presented explicitly in Eqs. (B9)-(B11). As W_{ij} describes the effective interaction (energetic + entropic) between two nonbonded monomers, the W_{ij} for a long chain system becomes independent of the chain size r_T. The chains then experience $\left|S_{ij}^{0^{-1}}\right| << \left|\beta W_{ij}\right|$ because $S_{ij}^{0^{-1}}$ scales as $1/r_T$. It can be seen for high polymers that $\Gamma_{11} - \Gamma_{22} \approx \beta(\bar{\varepsilon}_{11} - \bar{\varepsilon}_{22}) f_p u(\eta)/\eta$, where $u(\eta)=(\gamma/C)^4\eta^4-(\gamma/C)^2\eta^2$ with $\gamma = 1/\sqrt{2}$ and C = π/6 describes the packing density dependence of attractive nonbonded interactions and f_p = 4 is a numeric prefactor associated with $u(\eta)$, as seen in Appendix A. As all the monomer diameters are identical, difference in compressibility between constituents is described solely by difference in self-interaction parameters $\bar{\varepsilon}_{ii}$'s. A constituent with larger $\bar{\varepsilon}_{ii}$ is less compressible. Therefore, $\Gamma_{11} - \Gamma_{22}$ or equivalently $\overline{\Gamma}_{12}\,(=\eta(\Gamma_{11} - \Gamma_{22})/2)$ implies the compressibility difference in the block copolymer system. [22]

It was shown in our previous communications[14,16] that $\overline{\Gamma}_{11} = \eta \cdot [2\chi_s - 2\chi_{app}]$, where $2\chi_s$ is the well-known Gaussian term (Eq. (III-22) in ref. 3) in Leibler's work, and χ_{app} is the exchange energy density defined as $\chi_{app} \equiv \beta \cdot [\bar{\varepsilon}_{11} + \bar{\varepsilon}_{22} - 2\bar{\varepsilon}_{12}] \cdot f_p/2 \cdot |u(\eta)|$. If we define χ_{comp} and χ_{cRPA} as $\chi_{comp} \equiv \overline{\Gamma}_{12}^2/2\eta\overline{\Gamma}_{22}$ and $\chi_{cRPA} \equiv \chi_{app} + \chi_{comp}$, respectively, then the Landau energy in Eq. (19) can be rewritten as

$$\beta\delta F = \eta\left[2\chi_s - 2\chi_{cRPA}\right]\cdot\overline{\psi}_n(1)^2 - \left[\frac{\eta a_n}{r_T} + \frac{\Delta\overline{\Gamma}_{12}}{\overline{\Gamma}_{22}}\right]\overline{\psi}_n(1)^3 + \left[\frac{\eta b_n}{r_T} - \frac{\Delta^2}{4\overline{\Gamma}_{22}^{(2)}} - \frac{\Pi^2}{4\overline{\Gamma}_{22}^{(2)}(2q^*)}\right]\overline{\psi}_n(1)^4 \quad (20)$$

Spinodals are determined by vanishing quadratic term of the free energy in Eq. (20), which yields $\chi_{cRPA}(q^*) = \chi_s(q^*)$. Because $\chi_s(q^*)$ is purely given from the Gaussian characteristics, it is only dependent on r_T and ϕ_i. This procedure suggests that the newly defined χ_{cRPA} together with the chain size r_T serves a role of relevant parameter for spinodals in compressible block copolymers. It can be easily seen that the mean-field spinodal condition gives $\chi_{cRPA}(q^*) = 10.495/r_T$ universally for a symmetric copolymer. [23]

As PA and PB in Table I possess the same homopolymer molecular parameters, the diblock copolymer from PA (component 1) and PB (2), denoted as PA-*b*-PB, does not have compressibility difference between blocks. As $\bar{\varepsilon}_{11} = \bar{\varepsilon}_{22}$, $\overline{\Gamma}_{12}$ and thus χ_{comp} vanish. The ζ_n correspondingly vanishes. There is only a need for $\overline{\psi}_n(1)$ and ξ_n. In this case, the Landau free energy in Eq. (20) reduces to the free energy formulated in our previous work,[14,16] which simply replaces Flory χ with the density dependent χ_{app}:

$$r_T\beta\delta F/\eta \approx r_T\left[2\chi_s - 2\chi_{app}\right]\cdot\overline{\psi}_n(1)^2 - a_n\overline{\psi}_n(1)^3 + b_n\overline{\psi}_n(1)^4 \quad (21)$$

It can be said that this equation takes Leibler's expression as its limiting case ($\eta \to 1$). The resultant phase diagram is therefore identical to that from Leibler's theory if we use χ_{app} instead. Order-disorder (ODT) and order-order (OOT) transition temperatures along with spinodals are monotonically increasing with the increase of pressure due to

the increased density. Block copolymers exhibiting this type of phase behavior are the most common polystyrene-*b*-polybutadiene (PS-*b*-PBD) [24] and polystyrene-*b*-polyisoprene (PS-*b*-PI). [25] Figure 2 shows the phase diagram in terms of the relevant parameter $r_T\chi_{app}$ against composition for PA-*b*-PB with r_T = 400 as an illustration and the pressure dependence of transition temperatures for the copolymer at ϕ_1 = 0.45. It should be recalled that there is a continuous transition or critical point for the symmetric copolymer in this mean-field phase diagram implying Ising universality class.

In our second situation, we consider the diblock copolymer from PA (1) and PC (2), denoted as PA-*b*-PC, where there is an appreciable compressibility difference between blocks ($[\bar{\varepsilon}_{11}-\bar{\varepsilon}_{22}]/k$ = 428.4 K). In this case, $\overline{\Gamma}_{12}$ ($\approx \beta(\bar{\varepsilon}_{11}-\bar{\varepsilon}_{22})\cdot f_p/2\cdot u(\eta)$) becomes negative because $u(\eta)$ is negative in the useful η range. The Landau free energy takes all the terms in Eq. (20) due to the presence of negative $\overline{\Gamma}_{12}$. The phase diagram for this copolymer with r_T = 400 in terms of the relevant parameter, $r_T\chi_{cRPA}$ in this case, is plotted as a function of composition ϕ_1 in Fig. 3a. Table II lists all the order parameter amplitudes and Δ at ODT as a function of composition ϕ_1 for the copolymer. The small ζ_n shown in this table suffices the imposed condition that ζ_n is of order $\overline{\psi}_n(1)^2$. It can be seen in this plot that there is no continuous transition for the symmetric copolymer with nonvanishing $\overline{\psi}_n(1)$ and other two. This result is caused by the fact that $-\Delta\overline{\Gamma}_{12}/\overline{\Gamma}_{22}$ gives nonvanishing and negative, even though slight, contribution to the free energy for bcc and hex morphologies, as is shown in Table II. The sequence of transition is $\text{lam}\rightarrow\text{hex}\rightarrow\text{bcc}\rightarrow\text{disorder}$ upon heating for the entire range of composition. The effective Flory-type $\chi_{cRPA}(q^*)$ at ODT for the symmetric copolymer is found to be $10.4936/r_T$ ($<10.495/r_T$), whereas that at spinodal is exactly

$10.495/r_T$ as it should. A similar feature has already been demonstrated in our previous work on LDOT systems, where χ_{app} is negative and the microphase separation is driven by compressibility difference.[13] It is thus clear that block copolymers with finite compressibility difference do not belong to Ising universality class even in the mean-field situation. The presence of appreciable compressibility difference yields the anomalous pressure dependence of the transition temperatures. In plot b of Fig. 3, the transition temperatures for the copolymer at ϕ_1 = 0.45 show apparent decrease upon pressurization. This result can be explained by the fact that the applied pressure suppresses the compressibility difference. This action in turn suppresses $\overline{\Gamma}_{12}$ or χ_{comp}, which then enhances miscibility. Poly(ethylethylene)-*b*-poly(ethylene-propylene) (PEE-*b*-PEP) in fact revealed such pressure dependence of the observed transition temperatures. [26]

The diblock copolymer from PA (1) and PD (2), which is denoted as PA-*b*-PD, exhibits a similar phase diagram to PA-*b*-PC. The chain sizes are set to r_T = 400 again. However, somewhat reduced compressibility difference ($\left[\bar{\varepsilon}_{11} - \bar{\varepsilon}_{22}\right]/k$ = 379.4 K) renders the system possessing more complicated pressure dependence of transition temperatures. The ODT, OOT, and spinodals for PA-*b*-PD at ϕ_1 = 0.45 shown in Fig. 4 first decrease and then increase with the increase of pressure. This result can be interpreted as the response of χ_{app} and χ_{comp} upon pressurization in a reverse way to each other. The applied pressure first suppresses χ_{comp} to cause enhanced miscibility, and then the increased χ_{app} due to the density increase overtakes χ_{comp} to hamper miscibility. In addition, $\chi_{cRPA}(q^*)$ at ODT for the symmetric PA-*b*-PD, which is $10.4939/r_T$, is closer to the spinodal value than that for the symmetric PA-*b*-PC. This result is harmonious with the fact that compressibility difference in the PA-*b*-PD system

is smaller than that in the previous case. It was reported by Schwahn and co-workers that poly(ethylene-propylene)-*b*-poly(dimethyl siloxane) (PEP-*b*-PDMS) and poly(ethylethylene)-*b*-poly(dimethyl siloxane) (PEE-*b*-PDMS) indeed revealed such a peculiar pressure response. [27,28]

In our previous publications, the phase behavior of PS-*b*-PBD and PS-*b*-PI as real examples of PA-*b*-PB with vanishingly small χ_{comp} has been analyzed. [14,16] Here, we present the analyses of PEE-*b*-PEP and PEE-*b*-PDMS as examples of PA-*b*-PC and PA-*b*-PD, respectively. Table III shows two sets of three molecular parameters which best fit the volumetric properties of hydrogeneous PEE and PEP[29] to the CS equation of state. The cross-contact interaction $\bar{\varepsilon}_{PEE-PEP}$, or the resultant exchange energy $\Delta\bar{\varepsilon}$, is obtained from fitting the calculated mean-field ODT to the experimental value of the copolymer with molecular weight of 53600 at ϕ_{PEE} = 0.44, which is reported as 369 K by Bates and co-workers. [30,31] In Fig. 5, the calculated ODT is plotted as a function of pressure. It is found that the theory predicts the slow increase of the ODT and OOT with the pressure increase (7 – 8 K/100 MPa) due to the smallness of $(\bar{\varepsilon}_{PEE} - \bar{\varepsilon}_{PEP})/k = 106.8K$ or weak χ_{comp}. However, Schwahn and co-workers reported that the partially deuterated PEE-*b*-PEP copolymer having the total degree of polymerization of 1100 with 35% of PEE block showed the decreasing tendency of ODT upon pressurization (-17 K/100 MPa), but no apparent change in OOT. [26] It can be seen in Fig. 5 that the observed pressure dependence of ODT requires the increase of χ_{comp} from changing $\bar{\varepsilon}_{ii}$'s by ~1% to have $(\bar{\varepsilon}_{PEE} - \bar{\varepsilon}_{PEP})/k = 161.46K$. The necessary changes in $\bar{\varepsilon}_{ii}$'s may be in part attributed to the uneven deuteration of PEE and PEP, where 25 % of hydrogen is deuterated for the former polymer but 50% for the latter. The difference $\bar{\varepsilon}_{PEE} - \bar{\varepsilon}_{PEP}$ is increased in this situation because deuteration would in

general reduce $\bar{\varepsilon}_{ii}$.[32] Additional creation of voids in mixing PEE and PEP due to the structural difference between the two may also be a possibility. It is another factor that the inaccuracy involved in volumetric data may introduce the uncertainty in molecular parameters.

The molecular parameters for PEE/PDMS systems are shown in Table IV. Those parameters for PDMS are again obtained from fitting the volumetric data of the hydrogeneous PDMS [33] to the CS equation of state. The cross-contact interaction $\bar{\varepsilon}_{PEE-PDMS}$ in this table has been obtained from fitting the cloud point of near symmetric blends of partially deuterated PEE and hydrogeneous PDMS, measured by Schwahn and co-workers, [28,34] to the theoretical spinodal by using Eq. (A4). Figure 6 shows the calculated ODT as a function of pressure for the PEE-*b*-PDMS copolymer with the degree of polymerization of 84 for each block. It is seen that the theory predicts a somewhat rapid decrease of the ODT upon pressurization even with the fully ordered state, i.e., hourglass behavior, at 0.1 MPa due to the input compressibility difference, which is $(\bar{\varepsilon}_{PEE} - \bar{\varepsilon}_{PDMS})/k = 633.2K$. The experimental ODT of the copolymer with the partially deuterated PEE block and also cloud points of the corresponding blends tend first to decrease upon pressurization up to ~50 MPa, and then to increase, [28] as seen in Fig. 6. In order to best represent the experimental situation for the block copolymers and the blends, the compressibility difference or χ_{comp} has to be reduced as $\bar{\varepsilon}_{ii}$'s are changed by 5 - 6 percent. This situation is also drawn in the figure. PEE and PDMS in a mixture seem to feel less compressibility difference than expected, even though there may again be deuteration effects and inaccuracy involved in volume data. The partial deuteration of PEE would at least help to reduce $\bar{\varepsilon}_{PEE} - \bar{\varepsilon}_{PDMS}$.

Hereto, we have shown various phase behavior of UODT diblock copolymers. The

consideration of three hypothetical block copolymer systems and several real systems enables us to clearly assign molecular origin to microphase transitions and their pressure responses of most UODT copolymers at least in the mean-field sense. It is believed that the pressure response of transition temperatures is a precise measure of compressibility difference felt by block copolymers because the phase behavior of UODT systems is sensitive to slight changes in interaction parameters.

IV. CONCLUDING REMARKS

A new Landau free energy, Eq. (19) or (20), has been derived for diblock copolymers exhibiting UODT behavior. Compressibility difference between constituent blocks is generally allowed in the formulation of the free energy. The resultant Landau energy takes Leibler's incompressible version and that with no compressibility difference, which was previously suggested by the present author, as its limiting cases. The quadratic term of the Landau energy naturally yields the definition of an effective Flory-type interaction, χ_{cRPA}, which can be divided into the exchange energy density χ_{app} and a new χ_{comp} ($\propto \overline{\Gamma}_{12}^2$) characterizing the compressibility difference. In the cubic term, there is an additional contribution from $\overline{\Gamma}_{12}$ which gives a first-order transition for a symmetric copolymer even in the mean-field situation provided that there is appreciable compressibility difference. The phase behavior of typical UODT diblock copolymers is analyzed. Conventional and anomalous responses of ODT, OOT, and spinodals to pressure for those copolymers are analyzed through our Landau energy and χ_{cRPA}.

Finally, the formulated Landau free energy may be used as a reference free energy for the Hartree analysis[5,6] in order to consider concentration fluctuation effects on the phase behavior of compressible UODT block copolymers, which is the subject of our future

study.

ACKNOWLEDGMENTS

This work has been supported by Korea Science and Engineering Foundation through Hyperstructured Organic Materials Research Center (HOMRC). The author acknowledges S. I. Chang and J. S. Kim for their assistance in numerical calculations and preparing some of the figures.

APPENDICES

APPENDIX A. CHO-SANCHEZ EQUATION-OF-STATE MODEL AND SPINODALS

In this appendix, the Cho-Sanchez (CS) equation-of-state model is briefly introduced. The CS model was originally developed for polymer blends. [12,18] A binary blend system of two polymers consists of N_1 chains of r_1-mers and N_2 chains of r_2-mers. Each polymer chain in the system is simplified to be the linear chain of tangent spherical monomers that have the identical diameter σ.

The CS model suggests the free energy as $A = A_0^{id} + A_0^{EV} + U^{nb}$. The A_0^{id} represents the ideal free energy of the noninteracting Gaussian blend system. The A_0^{EV} and U^{nb} stand for the contribution to the free energy from the excluded volume effects and the attractive interactions between nonbonded monomers, respectively. Each term of the free energy is written explicitly in the following analytical equation:

$$\frac{\beta A}{rN} = \sum \frac{\phi_i}{r_i} \ln \frac{\eta \phi_i I_i \Lambda_i^{3r_i}}{r_i \mathrm{v}^* z_i e} + \left\{ \frac{3}{2} \left[\frac{1}{(1-\eta)^2} - \left(1 - \frac{1}{r}\right) \frac{1}{1-\eta} \right] - \frac{1}{r} \left[\ln(1-\eta) + \frac{3}{2} \right] \right\} + \frac{f_p}{2} \cdot \beta \bar{\varepsilon} \cdot u(\eta) \tag{A1}$$

where v* ($= \pi\sigma^3/6$) is the volume of one monomer. In Eq. (A1), $N=N_1+N_2$ is the total number of chains and $r = (r_1 N_1 + r_2 N_2)/N$ denotes the average chain size. The ϕ_i is the close-packed volume fraction of *i*-monomers, and thus $\phi_i = r_i N_i / rN$. The Λ_i and I_i imply the thermal de Broglie wavelength of monomers on *i*-chains and the symmetry number of *i*-chains, respectively. The symbol z_i implies the conformational partition function of Gaussian *i*-chains, which will be left as an unspecified constant here. The transcendental number *e* equals 2.718 and β is *1/kT* as usual. The η denotes the total packing density that implies the fraction of volume occupied by all the chains.

The $u(\eta)$ in Eq. (A1) describes the packing density dependence of attractive nonbonded interactions as

$$u(\eta) = \left[(\gamma / C)^{p/3} \eta^{p/3} - (\gamma / C)^2 \eta^2 \right] \tag{A2}$$

where $\gamma = 1/\sqrt{2}$, $C = \pi/6$, and $p = 12$. The $u(\eta)$ originates in the Lennard-Jones (L-J) potential acting between two monomers. The f_p in Eq. (A1) is a numeric prefactor associated with the L-J potential, and simply $f_p = 4$. The parameter $\bar{\varepsilon}$, defined as $\bar{\varepsilon} = \sum_{ij} \phi_i \phi_j \cdot \bar{\varepsilon}_{ij}$, describes the characteristic energy of the blend, where $\bar{\varepsilon}_{ij}$ implies the

L-J potential depth of the attractive interactions between two monomers on *i* and *j*-chains.

To apply the free energy in Eq. (A1) to a specific blend system, one requires various molecular parameters such as $\bar{\varepsilon}_{ii}$, r_i, and σ for given homopolymers and $\bar{\varepsilon}_{ij}$ for cross interactions between different homopolymers. Homopolymer parameters can be obtained from fitting measured volumetric data to the following equation of state:

$$\eta^2 \frac{\partial A}{\partial \eta} = r_T N \mathrm{v} * P \tag{A3}$$

The cross-interaction parameter $\bar{\varepsilon}_{ij}$ is commonly estimated as $\bar{\varepsilon}_{ij} = \xi\left(\bar{\varepsilon}_{ii}\bar{\varepsilon}_{jj}\right)^{1/2}$ with an adjustable parameter ξ, which can be determined from various mixture behavior such as the following spinodal condition:

$$g_{\phi\phi}/kT = \frac{1}{r_1\phi_1} + \frac{1}{r_2\phi_2} - 2\left[\chi_{app} + \frac{v^*\kappa_T}{2\eta kT}P_\phi^2\right] \tag{A4}$$

where χ_{app} is already defined in the main text and κ_T is the isothermal compressibility. The P_ϕ describes the compressibility difference between constituents, which can be written explicitly as

$$P_\phi v^*/kT = \frac{f_p}{2}\left\{\beta\bar{\varepsilon}_{11} - \beta\bar{\varepsilon}_{22} - \chi(1-2\phi_1)\right\}\cdot\eta^2\frac{\partial u(\eta)}{\partial\eta} + \left(\frac{1}{r_1} - \frac{1}{r_2}\right)\left[\frac{3}{2}\frac{\eta^2}{(1-\eta)^2} + \frac{\eta^2}{1-\eta} + \eta\right] \tag{A5}$$

From Eq. (A4), it can be easily seen that the compressibility term always hampers miscibility because it is always negatively contributing to spinodal condition.

APPENDIX B. COMPRESSIBLE RPA

A RPA is an approximation method to calculate the second-order monomer-monomer correlation function $G_{ij}^{(2)}$, or equivalently S_{ij}, and higher-order correlation functions $G^{(n)}$'s for the analysis of phase segregation in polymer blends and block copolymers. [3,4] Recently, the present author successfully combined the RPA with CS equation-of-state model to analyze compressibility effects. [12-16]

The basic idea of the theory follows the spirit of the incompressible RPA by Leibler. A phase segregating system is characterized by the so-called order parameter ψ_i ($\equiv \langle \eta_i(\vec{r}) - \eta_i \rangle$), which is defined as the thermal average of the difference between the local density $\eta_i(\vec{r})$ and the global density η_i of *i*-monomers. The Landau expansion of the free energy is expressed as a series in the order parameter ψ_i, where the coefficients in the Landau expansion are called the vertex functions $\Gamma^{(n)}$. The ψ_i can also be expanded as a series in U_i, which is conjugate to the order parameter ψ_i. The coefficients appearing in the series for ψ_i are the correlation functions $G^{(n)}$'s. In estimating ψ_i, the correlation functions $G^{(n)}$ are supposed to be equal to those of noninteracting Gaussian copolymer chains, which are denoted as $G^{(n)0}$. The external potential U_i is then substituted with U_i^{eff}, which is corrected as $U_i^{eff} = U_i + W_{ij}\psi_j$ to properly take the interaction effects into account by an interaction field W_{ij}. The W_{ij} replaces the simple Flory-Huggins χ to account for the desired compressibility effects,

and is formulated from the CS model. The resultant self-consistent field equation is solved in an iterative technique to obtain correlation functions. [13] The correlation functions then yield the vertex functions as seen in our previous study. The second-order vertex function is only written here for example as

$$\Gamma_{ij}^{(2)} = S_{ij}^{-1} = S_{ij}^{0\,-1} + \beta W_{ij} \tag{B1}$$

It should be kept in mind that the vertex functions $\Gamma^{(n)}(\vec{q}_1,...,\vec{q}_n)$ are nonvanishing only if $\sum_{i=1}^{n}\vec{q}_i$ vanishes.

For the analysis of compressible UODT diblock copolymer systems, it is more convenient to use the following order parameter $\overline{\psi}_i$ instead of the original ψ_i:[14]

$$\overline{\psi}_i = M_{ij}\psi_j \tag{B2}$$

where M_{ij} is defined as

$$\left[M_{ij}\right] = \begin{bmatrix} \frac{1}{2\eta} & -\frac{1}{2\eta} \\ 1 & 1 \end{bmatrix} \tag{B3}$$

The vertex functions $\Gamma^{(n)}$ in the Landau expansion of the free energy in ψ_i is then replaced with the proper vertex function $\overline{\Gamma}^{(n)}$ for $\overline{\psi}_i$ as

$$\overline{\Gamma}^{(n)}_{i_1\cdots i_n} = \Gamma^{(n)}_{j_1\cdots j_n} M^{-1}_{j_1 i_1} \cdots M^{-1}_{j_n i_n} \tag{B4}$$

Here, the first three vertex functions $\overline{\Gamma}^{(n)}$'s are only written explicitly as

$$\left[\overline{\Gamma}^{(2)}_{ij}\right] = \begin{bmatrix} \eta^2\left(\Gamma^{(2)}_{11} - 2\Gamma^{(2)}_{12} + \Gamma^{(2)}_{22}\right) & \eta/2\cdot\left(\Gamma^{(2)}_{11} - \Gamma^{(2)}_{12}\right) + \eta/2\cdot\left(\Gamma^{(2)}_{12} - \Gamma^{(2)}_{22}\right) \\ \eta/2\cdot\left(\Gamma^{(2)}_{11} - \Gamma^{(2)}_{12}\right) + \eta/2\cdot\left(\Gamma^{(2)}_{12} - \Gamma^{(2)}_{22}\right) & \Gamma^{(2)}_{11}/4 + \Gamma^{(2)}_{12}/2 + \Gamma^{(2)}_{22}/4 \end{bmatrix} \tag{B5}$$

$$\overline{\Gamma}^{(3)}_{ijk}\left(\vec{q}_1,\vec{q}_2,\vec{q}_3\right) = -V_{mi}\left(\vec{q}_1\right) G^{(3)\,0}_{mno}\left(\vec{q}_1,\vec{q}_2,\vec{q}_3\right) V_{nj}\left(\vec{q}_2\right) V_{ok}\left(\vec{q}_3\right) \tag{B6}$$

$$\begin{aligned} \overline{\Gamma}^{(4)}_{abcd}\left(\vec{q}_1,\vec{q}_2,\vec{q}_3,\vec{q}_4\right) = \Big[\int d\vec{q} S^{0\,-1}_{ko}\left(\vec{q}\right)\Big\{ & G^{(3)\,0}_{ijk}\left(\vec{q}_1,\vec{q}_2,\vec{q}\right) G^{(3)\,0}_{opr}\left(-\vec{q},\vec{q}_3,\vec{q}_4\right) + \\ & G^{(3)\,0}_{ipk}\left(\vec{q}_1,\vec{q}_3,\vec{q}\right) G^{(3)\,0}_{ojr}\left(-\vec{q},\vec{q}_2,\vec{q}_4\right) + G^{(3)\,0}_{irk}\left(\vec{q}_1,\vec{q}_4,\vec{q}\right) G^{(3)\,0}_{ojp}\left(-\vec{q},\vec{q}_2,\vec{q}_3\right)\Big\} - \\ & G^{(4)\,0}_{ijpr}\left(\vec{q}_1,\vec{q}_2,\vec{q}_3,\vec{q}_4\right)\Big] V_{ia}\left(\vec{q}_1\right) V_{jb}\left(\vec{q}_2\right) V_{pc}\left(\vec{q}_3\right) V_{rd}\left(\vec{q}_4\right) \end{aligned} \tag{B7}$$

where a new tensor V_{ij} in Eqs. (B6) and (B7) is defined as the combination of $S^{0\,-1}_{ij}$ and M_{ij} as

$$\left[V_{ij}\right] \equiv \left[S^{0\,-1}_{ik} M^{-1}_{kj}\right] = \begin{bmatrix} \eta\left(S^{0\,-1}_{11} - S^{0\,-1}_{12}\right) & \phi_1 S^{0\,-1}_{11} + \left(1-\phi_1\right) S^{0\,-1}_{12} \\ \eta\left(S^{0\,-1}_{21} - S^{0\,-1}_{22}\right) & \phi_1 S^{0\,-1}_{21} + \left(1-\phi_1\right) S^{0\,-1}_{22} \end{bmatrix} \tag{B8}$$

It should be noted that V_{i1} in Eq. (B8) is independent of η because $S^{0\,-1}_{ij}$ is proportional to $1/\eta$. The V_{i1} is indeed frequently employed to obtain higher-order

vertex functions Γ_3 and Γ_4 in the incompressible RPA by Leibler. [3]

Among various $\overline{\Gamma}^{(n)}$'s, $\overline{\Gamma}^{(3)}_{111}$ and $\overline{\Gamma}^{(4)}_{1111}$ are of our special interest. As seen in Eqs. (B6) and (B7), only V_{i1} is used to calculate those two vertex functions. It can then be easily seen that $\overline{\Gamma}^{(3)}_{111}$ and $\overline{\Gamma}^{(4)}_{1111}$ become identical with $\eta\Gamma_3$ and $\eta\Gamma_4$, i.e., the product of the packing density η and Leibler's vertex functions Γ_3 and Γ_4, respectively.

The interaction field W_{ij} is obtained from the nonideal free energy, $A_0^{EV} + U^{nb}$, of the CS model. The W_{ij} then consists of the two terms L_{ij} and ε_{ij}^{app}, which are formulated from A_0^{EV} and U^{nb}, respectively:

$$\beta W_{ij} = L_{ij}(\eta) - \beta\varepsilon_{ij}^{app}(\eta) \tag{B9}$$

where L_{ij} and ε_{ij}^{app} are given as

$$\begin{aligned} L_{ij}(\eta) = \frac{3}{2}\left[\frac{4}{(1-\eta)^3} + \frac{6\eta}{(1-\eta)^4} - (2 - \frac{1}{r_i} - \frac{1}{r_j})\frac{1}{(1-\eta)^2} - (\eta - \frac{\eta}{r})\frac{2}{(1-\eta)^3}\right] \\ + (\frac{1}{r_i} + \frac{1}{r_j})\frac{1}{1-\eta} + \frac{\eta}{r}\frac{1}{(1-\eta)^2} \end{aligned} \tag{B10}$$

and

$$-\beta\varepsilon_{ij}^{app}(\eta)=\beta\bar{\varepsilon}_{ij}f_p\frac{u(\eta)}{\eta}+\beta\left(\sum_k\eta_k\left\{\bar{\varepsilon}_{ik}+\bar{\varepsilon}_{jk}\right\}\right)f_p\frac{\partial}{\partial\eta}\left(\frac{u(\eta)}{\eta}\right)$$
$$+\frac{1}{2}\beta\left(\sum_{kl}\eta_k\eta_l\bar{\varepsilon}_{kl}\right)f_p\frac{\partial^2}{\partial\eta^2}\left(\frac{u(\eta)}{\eta}\right) \qquad \text{(B11)}$$

The interaction field W_{ij} given above was first derived for polymer blends with the close-packed volume fraction ϕ_i of *i*-monomers. The W_{ij} for polymer blends is then adopted for the corresponding block copolymers with the same ϕ_i.[12-16]

1 S. L. Aggarwal, *Block Copolymers*. (Plenum Press, New York, 1970); *Developments in Block Copolymers-I*, edited by I. Goodman (Applied Science Publishers, New York, 1982); *Thermoplastic Elastomers*, edited by G. Holden, N. R. Legge, R. P. Quirk, and H. E. Schroeder (Hanser, New York, 1996); T. S. Bailey, C. M. Hardy, T. H. Epps, and F. S. Bates, Macromolecules **35**, 7007 (2002).

2 I. W. Hamley, *The Physics of Block Copolymers*. (Oxford University Press, Inc., New York, 1998).

3 L. Leibler, Macromolecules **13**, 1602 (1980).

4 P.-G. de Gennes, *Scaling Concepts in Polymer Physics*. (Cornell University Press, Ithaca, N.Y., 1979).

5 G. H. Fredrickson and E. Helfand, J. Chem. Phys. **87**, 697 (1987).

6 A. M. Mayes and M. Olvera de la Cruz, J. Chem. Phys. **95(6)**, 4670 (1991).

7 J. Dudowicz and K. F. Freed, Macromolecules **26**, 213 (1993); J. Dudowicz and K. F. Freed, Macromolecules **28**, 6625 (1995); K. F. Freed and J. Dudowicz, J. Chem. Phys. **97**, 2105 (1992); W. E. McMullen and K. F. Freed,

Macromolecules **23**, 255 (1990); H. Tang and K. F. Freed, J. Chem. Phys. **94**, 1572 (1991); J. Dudowicz and K. F. Freed, Macromolecules **33**, 5292 (2000).

[8] C. Yeung, R. C. Desai, A. C. Shi, and J. Noolandi, Phys. Rev. Lett. **72**, 1834 (1994); U. R. Bidkar and I. C. Sanchez, Macromolecules **28**, 3963 (1995); T. Hino and J. M. Prausnitz, Macromolecules **31**, 2636 (1998).

[9] T. P. Russell, T. E. Karis, Y. Gallot, and A. M. Mayes, Nature **386**, 729 (1994); T. E. Karis, T. P. Russell, Y. Gallot, and A. M. Mayes, Macromolecules **28**, 1129 (1995); A.-V. G. Ruzette, P. Banerjee, A. M. Mayes, M. Pollard, T. P. Russell, R. Jerome, T. Slawecki, R. Hjelm, and P. Thiyagarajan, Macromolecules **31**, 8509 (1998); P. Mansky, O. K. C. Tsui, T. P. Russell, and Y. Gallot, Macromolecules **32**, 4832 (1999); D. Y. Ryu, U. Jeong, J. K. Kim, and T. P. Russell, Nature Mater. **1**, 114 (2002); D. Y. Ryu, U. Jeong, D. H. Lee, J. H. Kim, H. S. Youn, and J. K. Kim, Macromolecules **in press** (2003).

[10] T. Hashimoto, H. Hasegawa, T. Hashimoto, H. Katayama, M. Kamogaito, M. Sawamoto, and M. Imai, Macromolecules **30**, 6819 (1997).

[11] The latest reports by Kim and Russell[9] on immiscibility loop with both LDOT and UODT observed in the polystyrene-*b*-poly(n-pentyl methacrylate) melts raise a question about the origin of LDOT phenomena (compressibility difference or directional interaction) in this and other homologous block copolymers. A manuscript dealing with this topic is in preparation now.

[12] J. Cho, Macromolecules **33**, 2228 (2000).

[13] J. Cho, Macromolecules **34**, 1001 (2001).

[14] J. Cho, Macromolecules **34**, 6097 (2001).

[15] J. Cho, Polym. Prep. **41**, 1114 (2000).

[16] J. Cho, Macromolecules **35**, 5697 (2002).

[17] A. Z. Akcasu and M. Tombakoglu, Macromolecules **23**, 607 (1990); A. Z. Akcasu, R. Klein, and B. Hammouda, Macromolecules **22**, 1238 (1993).

[18] J. Cho and I. C. Sanchez, Macromolecules **31**, 6650 (1998).

[19] Olvera de la Cruz reported the failure in minimizing a Landau free energy and its Hartree correction in the incompressible situation for deep quenches if chain stretching is allowed, or in other words, the minimization procedure with respect to the scattering vector (q^*) is allowed. See: (a) M. Olvera de la Cruz, Macromolecules **24**, 3975 (1991). (b) M. Olvera de la Cruz, Phys. Rev. Lett. **95**, 1281 (1991).

[20] N. M. Maurits, B. A. C. van Vlimmeren, and J. G. E. M. Fraaije, Phys. Rev. E **56**, 816 (1997); J. G. E. M. Fraaije, B. A. C. van Vlimmeren, N. M. Maurits, M. Postma, O. A. Evers, C. Hoffmann, P. Altevogt, and G. Goldbeck-Wood, J. Chem. Phys. **106**, 4260 (1997).

[21] G. H. Fredrickson and L. Leibler, Macromolecules **22**, 1238 (1989).

[22] This $\overline{\Gamma}_{12} \approx \beta\left(\bar{\varepsilon}_{11} - \bar{\varepsilon}_{22}\right) \cdot f_p / 2 \cdot u(\eta)$ plays a similar role to P_ϕ of Eq. (A5) in the bulk thermodynamic spinodal condition.

[23] We have introduced a slightly different χ_{cRPA} in our previous publication.[16] These two χ_{cRPA}'s play a similar role, and indeed coincide at spinodals despite of differences in their mathematical expressions. The new χ_{cRPA} in Eq. (20) is also harmonious with the effective χ suggested by Yeung et al.[8]

[24] H. Ladynski, D. Odorico, and M. Stamm, J. Non-Cryst. Sol. **235-237**, 491 (1998); H. Frielinghaus, B. Abbas, D. Schwahn, and L. Willner, Europhys. Lett. **44 (5)**, 606 (1998).

[25] D. A. Hajduk, S. M. Gruner, S. Erramilli, R. A. Register, and L. J. Fetters, Macromolecules **29**, 1473 (1996).

[26] H. Frielinghaus, D. Schwahn, K. Mortensen, K. Almdal, and T. Springer, Macromolecules **29**, 3263 (1996).

[27] D. Schwahn, H. Frielinghaus, K. Mortensen, and K. Almdal, Phys. Rev. Lett. **77**, 3153 (1996).

[28] D. Schwahn, H. Frielinghaus, K. Mortensen, and K. Almdal, Macromolecules **34**, 1694 (2001).

[29] S. J. Han, D. J. Lohse, P. D. Condo, and L. H. Sperling, J. Polym. Sci.: Part B.: Polym. Phys. **37**, 2835 (1999).

[30] J. H. Rosedale, F. S. Bates, K. Almdal, K. Mortensen, and G. D. Wignall, Macromolecules **28**, 1429 (1995).

[31] It should be kept in mind that $\bar{\varepsilon}_{12}$ needs to be decreased a bit in order to reflect the fact that the concentration fluctuation effects lower the ODT from the mean-field value. It is seen that the increase of the mean-field ODT by ~100 K requires the decrease of $\bar{\varepsilon}_{12}$ by ~0.03 %.

[32] F. S. Bates, L. J. Fetters, and G. D. Wignall, Macromolecules **21**, 1086 (1988).

[33] *Polymer Handbook*, edited by J. Brandrup, E. H. Immergut, and E. A. Grulke (Wiley Interscience, New York, 1999).

[34] The blend of PEE and PDMS having the degrees of polymerization of 30.5 and 29.2, respectively, revealed the cloud point of 417 K.[28]

TABLE I. Molecular parameters for four hypothetical homopolymers and cross-interaction parameters for three pairs from PA and others.

Parameters	PA	PB	PC	PD
σ (Å)	4.04	4.04	4.04	4.04
$\bar{\varepsilon}_{JJ}/k$ (K)	4107.0	4107.0	3678.6	3727.6
$r/MW \cdot \pi\sigma^3/6$ (cm^3/g) [a]	0.41636	0.41636	0.41636	0.41636
$\bar{\varepsilon}_{AJ}/(\bar{\varepsilon}_{AA}\bar{\varepsilon}_{JJ})^{1/2}$	-	0.99534	0.99760	0.99708
$\Delta\bar{\varepsilon}/k$ (K)	-	38.277	30.452	32.042

[a] A composite parameter that yields the ratio of the chain size *r* to MW.

TABLE II. Various order parameter amplitudes and Δ in Eq. (15) tabulated against composition at the order-disorder transition for the PA-*b*-PC system.

ϕ_{PA}	$\overline{\psi}_n(1)$	ζ_n	ξ_n	Δ
0.112	0.0224	7.0148E-05	2.6870E-07	-0.4912
0.202	0.0378	2.5048E-04	8.8554E-07	-0.1903
0.301	0.0472	4.5860E-04	1.6353E-06	-0.1134
0.400	0.0385	4.5351E-04	1.2207E-06	-0.0877
0.500	0.0049	6.1683E-05	2.0523E-08	-0.0811
0.598	0.0388	4.7039E-04	1.3756E-06	-0.1025
0.697	0.0486	5.0097E-04	2.5456E-06	-0.1999
0.796	0.0388	2.8486E-04	2.1317E-06	-0.6092
0.887	0.0227	8.6578E-05	1.1760E-06	-3.4004

[a] Pressure is set to 0.1 MPa.

TABLE III. Molecular parameters for PEE-*b*-PEP systems

Parameters	PEE	PEP
σ (Å) [a]	3.820	3.657
$\bar{\varepsilon}/k$ (K)	2983.60 (+27.33)	2876.80 (-27.33)
$r/MW \cdot \pi\sigma^3/6$ (cm^3/g)	0.48757	0.48661
$\bar{\varepsilon}_{AB}/(\bar{\varepsilon}_{AA}\bar{\varepsilon}_{BB})^{1/2}$	0.99923 (0.99957)	
$\Delta\bar{\varepsilon}/k$ (K)	5.4850 (4.7436)	

[a] The slight discrepancy in monomer sizes σ's for the two polymers is resolved by employing the average $\sigma = (\sigma_1 + \sigma_2)/2$ for both.

[b] Numbers in the parentheses indicate the modification of parameters for PEE-*b*-PEP in order to represent the decreasing tendency of ODT upon pressurization reported by Schwahn and co-workers.[26]

[c] The necessary increase in $[\bar{\varepsilon}_{PEE} - \bar{\varepsilon}_{PEP}]/k$ ($106.8 \rightarrow 161.46$ K) is tentatively achieved by equally changing $\bar{\varepsilon}_{ii}$'s.

TABLE IV. Molecular parameters for PEE-*b*-PDMS systems

Parameters	PEE	PDMS
σ (Å)	3.820	3.774
$\bar{\varepsilon}/k$ (K)	2983.60 (-148.00)	2350.40 (+148.00)
$r/MW \cdot \pi\sigma^3/6$ (cm^3/g)	0.48757	0.41122
$\bar{\varepsilon}_{AB}/(\bar{\varepsilon}_{AA}\bar{\varepsilon}_{BB})^{1/2}$	1.00473 (0.99530)	
$\Delta\bar{\varepsilon}/k$ (K)	12.666 (35.689)	

[a] Numbers in the parentheses indicate the modification of parameters for PEE-*b*-PDMS in order to represent the peculiar behavior of ODT upon pressurization exhibiting a minimum reported by Schwahn and co-workers.[28]

[b] The requisite decrease in $[\bar{\varepsilon}_{PEE} - \bar{\varepsilon}_{PDMS}]/k$ ($633.2 \rightarrow 337.2$ K) is tentatively achieved again by equally changing $\bar{\varepsilon}_{ii}$'s.

Figure Captions

FIG. 1. Schematic behavior of the order parameters, $\overline{\psi}_1(\vec{r})$, $\zeta(\vec{r})$, and $\xi(\vec{r})$, along the direction perpendicular to lamellar layers. The $\overline{\psi}_1$ indicates the density fluctuations of A-block, which is taken as the less compressible component. The symbol ζ represents the free volume fluctuations due to the compressibility difference, whereas ξ implies those for the screening of unfavorable cross-contacts at the interfaces.

FIG. 2. Phase diagram (a) for PA-*b*-PB with r_T = 400 in terms of the relevant parameter $r_T \chi_{app}$ against ϕ_{PA}, and the pressure dependence (b) of transition temperatures for the copolymer at ϕ_{PA} = 0.45. The symbol T_s implies mean-field spinodals.

FIG. 3. Phase diagram (a) for PA-*b*-PC with r_T = 400 in terms of the relevant parameter $r_T \chi_{cRPA}(q^*)$ against ϕ_{PA}, and the pressure dependence (b) of transition temperatures for the copolymer at ϕ_{PA} = 0.45. It should be noted that there is no continuous transition and $r_T \chi_{cRPA}(q^*)$ = 10.4936 at ODT for the symmetric copolymer.

FIG. 4. Pressure dependence of ODT and OOT along with the mean-field spinodals for PA-*b*-PD at ϕ_{PA} = 0.45.

FIG. 5. ODT as a function of pressure for PEE-*b*-PEP with MW = 53600 at ϕ_{PEE} = 0.44 using the original set (open square) of molecular parameters and the modified one (open circle) in Table III. It should be remembered that the corresponding spinodals and

OOT exhibit the similar pressure dependence to the ODT drawn.

FIG. 6. ODT as a function of pressure for PEE-*b*-PDMS with the degree of polymerization of 84 for each block using the original set (open square) of molecular parameters and the modified one (open circle) in Table IV. Here, the experimental data (filled diamond) from ref. 28 are drawn together.

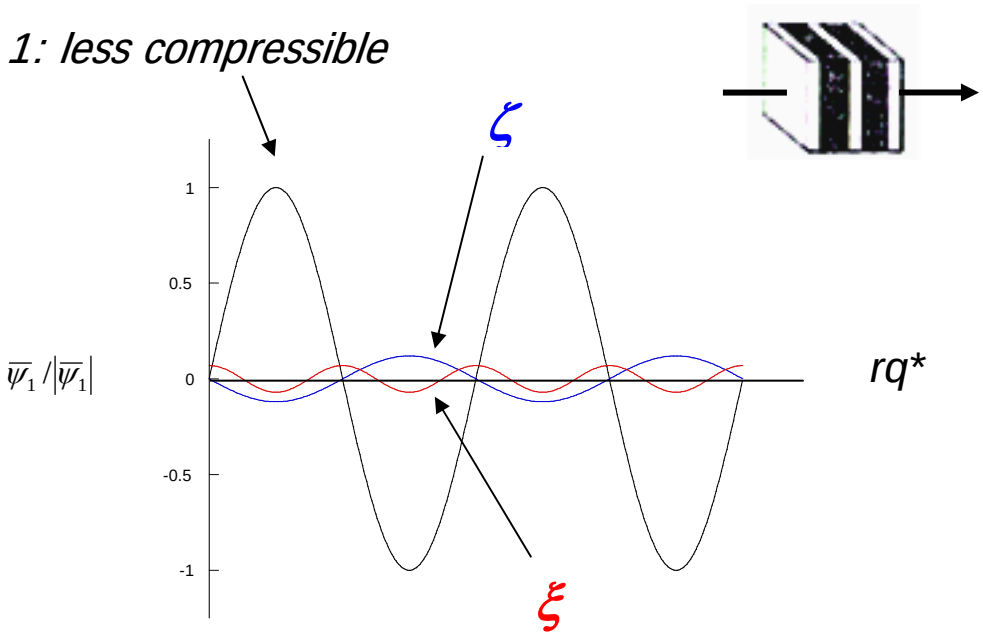
1: less compressible
ζ
1
0.5
0
-0.5
-1
$\overline{\psi}_1/|\overline{\psi}_1|$
rq*
ξ

J. Cho Fig. 1

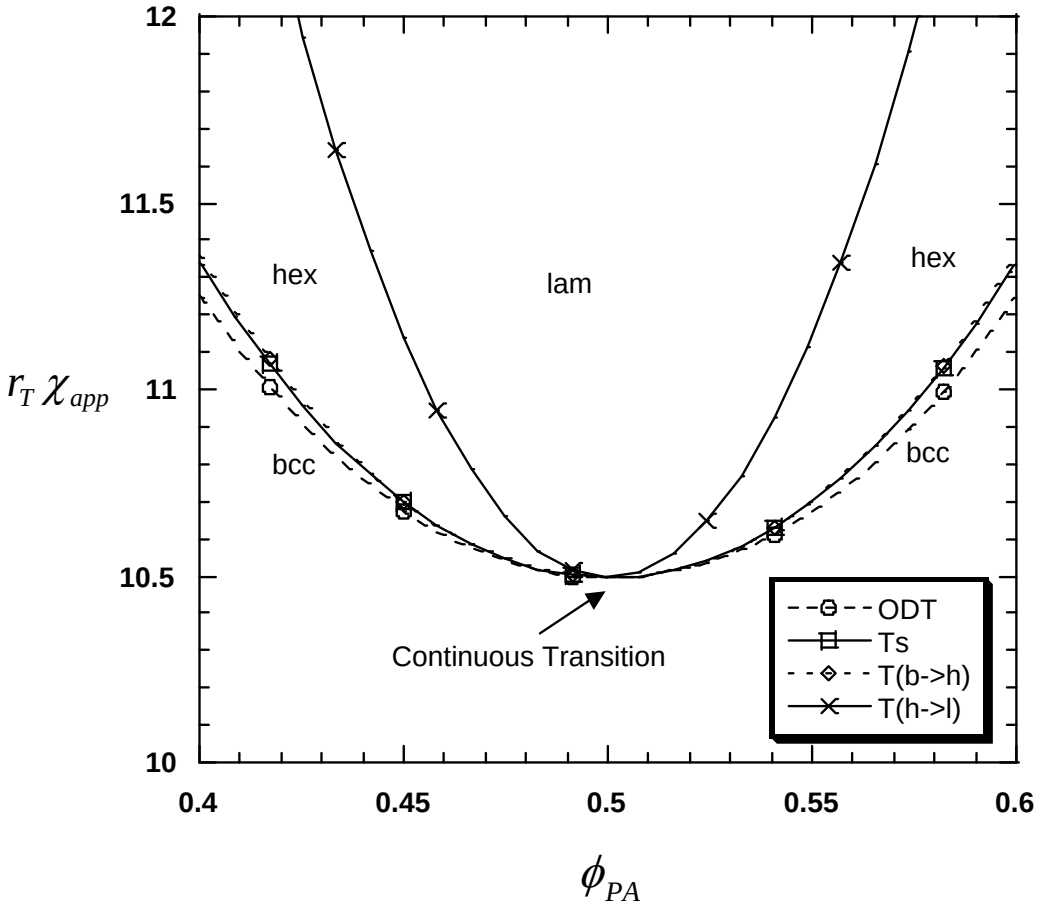
12
11.5
11
10.5
10
0.4
0.45
0.5
0.55
0.6
$r_T \chi_{app}$
ϕ_{PA}
hex
lam
hex
bcc
bcc
Continuous Transition
ODT
Ts
T(b->h)
T(h->l)

J. Cho Fig. 2a

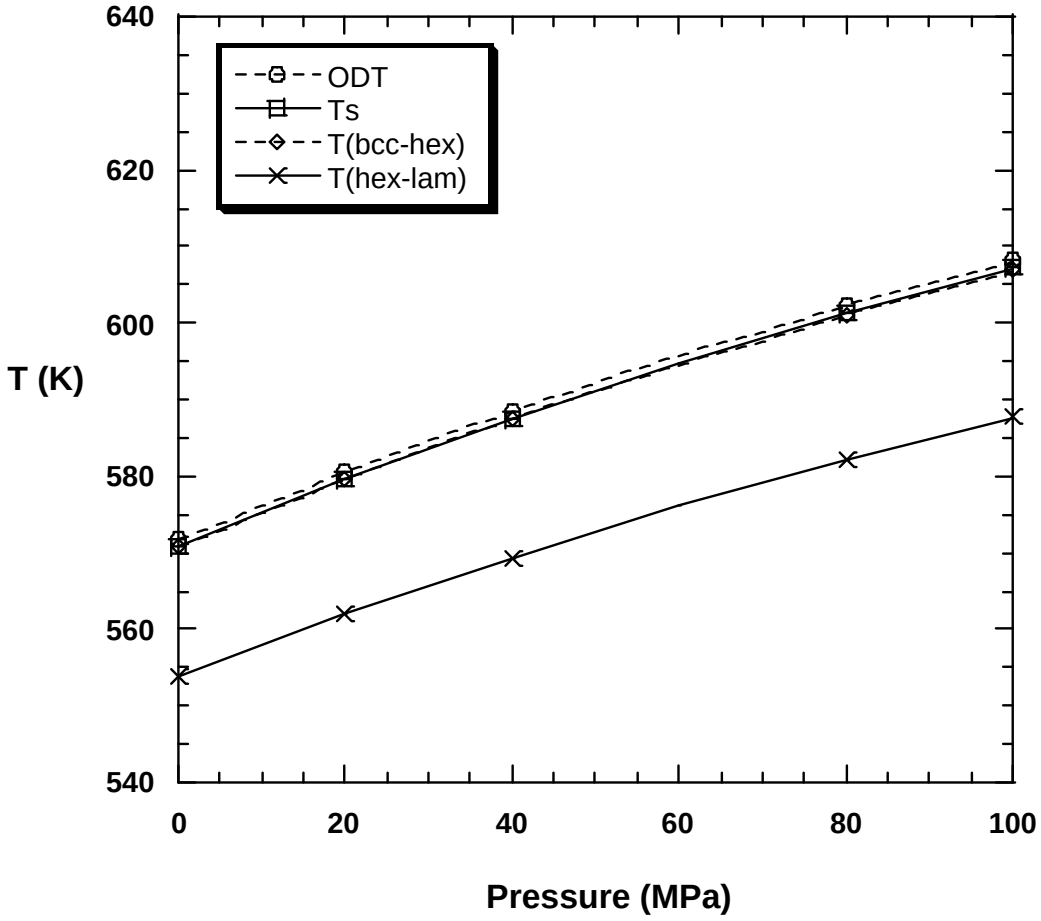
640
620
600
580
560
540
T (K)
0
20
40
60
80
100
Pressure (MPa)
ODT
Ts
T(bcc-hex)
T(hex-lam)

J. Cho Fig. 2b

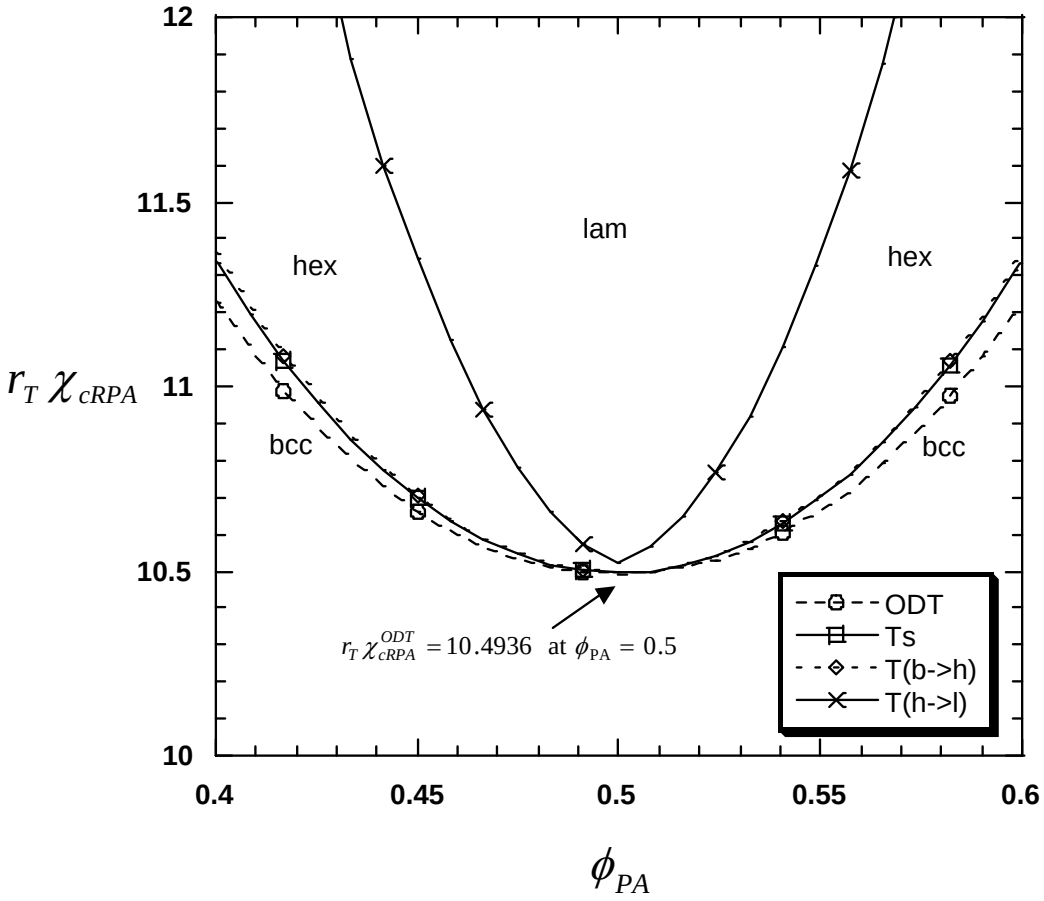
12
11.5
11
10.5
10
0.4
0.45
0.5
0.55
0.6
$r_T \chi_{cRPA}$
ϕ_{PA}
hex
lam
hex
bcc
bcc
$r_T \chi_{cRPA}^{ODT} = 10.4936$ at $\phi_{PA} = 0.5$
ODT
Ts
T(b->h)
T(h->l)

J. Cho Fig. 3a

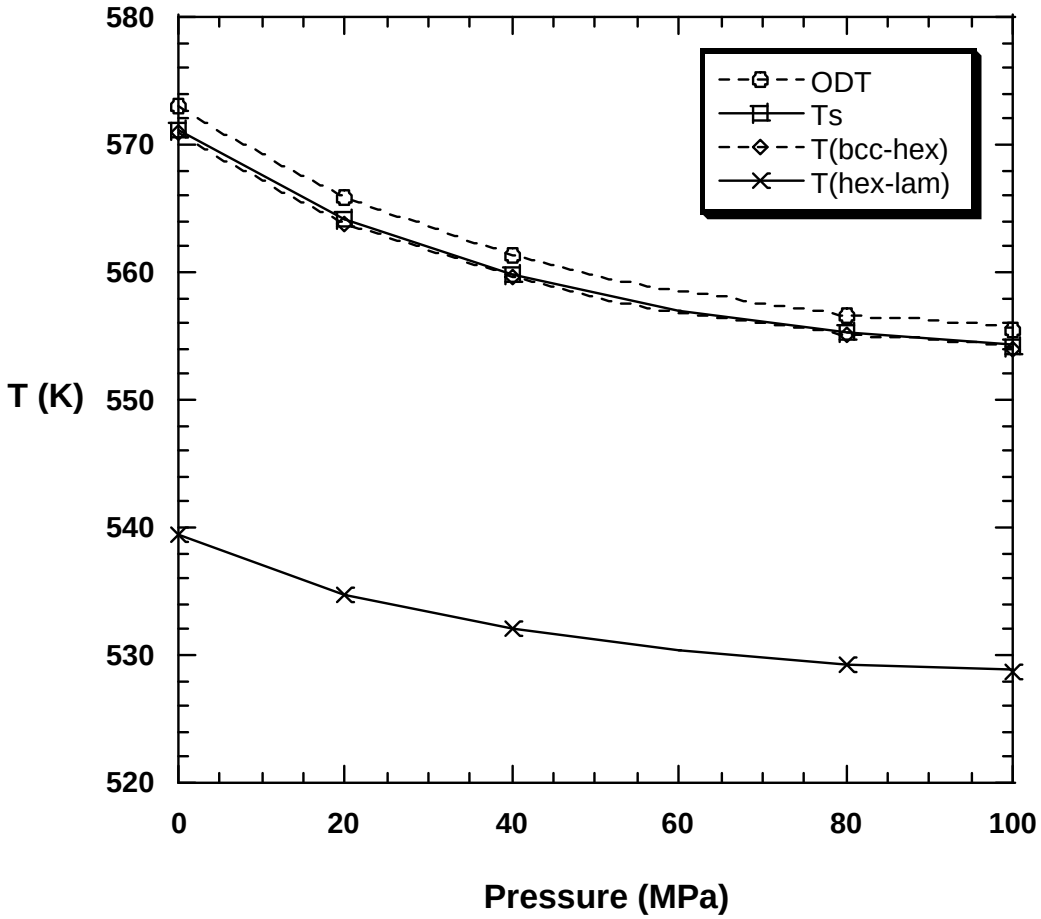
580
570
560
550
540
530
520
T (K)
0
20
40
60
80
100
Pressure (MPa)
ODT
Ts
T(bcc-hex)
T(hex-lam)

J. Cho Fig. 3b

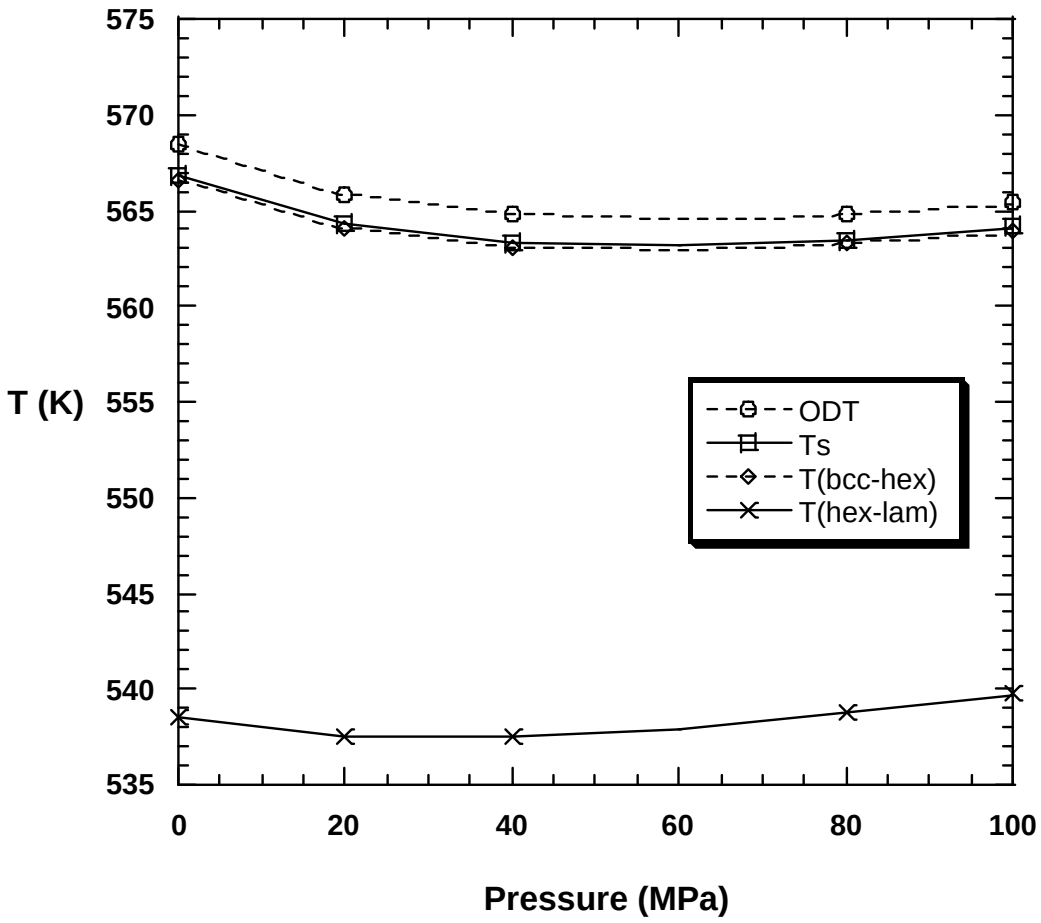
575
570
565
560
555
550
545
540
535
T (K)
0
20
40
60
80
100
Pressure (MPa)
ODT
Ts
T(bcc-hex)
T(hex-lam)

J. Cho Fig. 4

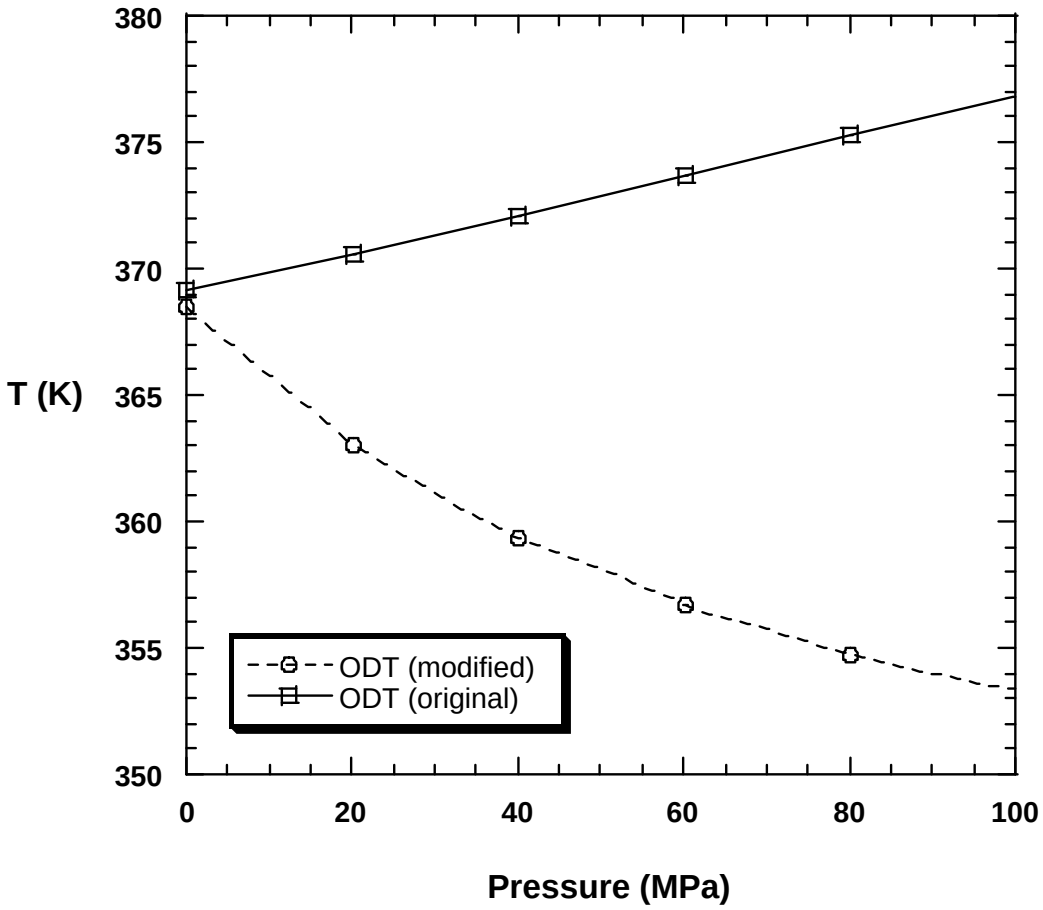
380
375
370
365
360
355
350
T (K)
0
20
40
60
80
100
Pressure (MPa)
ODT (modified)
ODT (original)

J. Cho Fig. 5

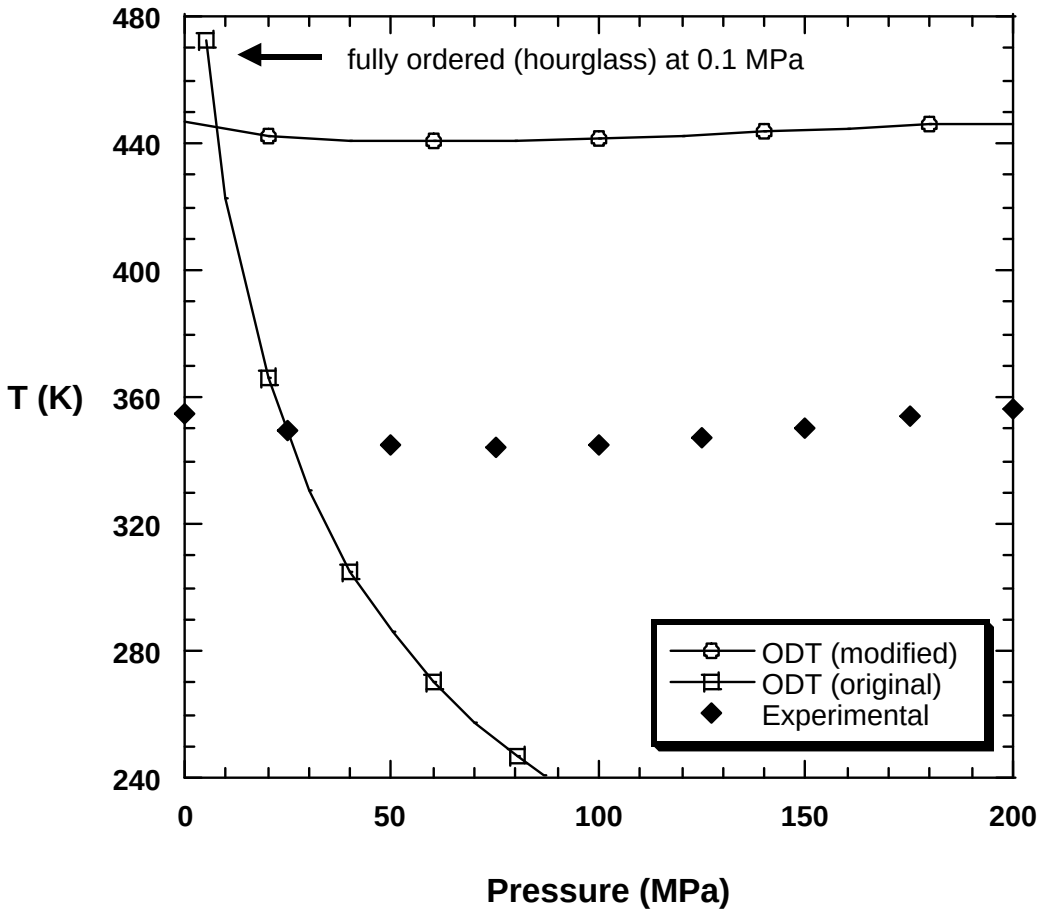
480
440
400
360
320
280
240
T (K)
0
50
100
150
200
Pressure (MPa)
fully ordered (hourglass) at 0.1 MPa
ODT (modified)
ODT (original)
Experimental

J. Cho Fig. 6